

Nanotubes in polar media: polarons and excitons on a cylinder

Yu. N. Gartstein,¹ T. D. Bustamante,¹ and S. Ortega Castillo²

¹*Department of Physics, The University of Texas at Dallas,
P. O. Box 830688, FO23, Richardson, Texas 75083, USA*

²*FAMAT, University of Guanajuato, Guanajuato, Mexico*
(Dated: October 23, 2018)

Electrons and holes on semiconducting nanotubes immersed in sluggish polar media can undergo self-localization into polaronic states. We evaluate the binding energy E_b^{pol} of adiabatic Fröhlich-Pekar polarons confined to a cylindrical surface and compare it to the corresponding exciton binding energy E_b^{exc} . The ratio $E_b^{\text{pol}}/E_b^{\text{exc}}$ is found to be a non-monotonic function of the cylinder radius R that can reach values of about 0.35, substantially larger than values of about 0.2 for $2d$ or $3d$ systems. We argue that these findings represent a more general crossover effect that could manifest itself in other semiconductor nanostructures in $3d$ polar environments. As a result of the strong polaronic effect, the activation energy of exciton dissociation into polaron pairs is significantly reduced which may lead to enhanced charge separation.

PACS numbers: 73.22.-f, 73.21.-b, 71.35.-y, 71.38.-k

I. INTRODUCTION

Low-dimensional semiconductor structures such as quantum wells, quantum wires, nanotubes and conjugated polymers are important for practical applications and interesting scientifically. It is known that the confinement of the motion of charge carriers in some directions leads to increased effects of the Coulomb interaction on system excitations. In this paper we are concerned with two types of such effects: *excitonic* and *polaronic*. The excitonic effect refers to the formation of Coulombically bound electron-hole pairs, Wannier-Mott excitons, which progressively affect optical properties of semiconductors: the exciton binding energy E_b^{exc} increases from its $3d$ value to $2d$ and, further on, to quasi- $1d$ magnitudes (E_b^{exc} diverges in pure $1d$).¹ The polaronic effect occurs in polar media, where the Coulomb field of an individual charge carrier causes the polarization (deformation) of its surroundings resulting in the carrier self-localization into polaronic states. Such polarons have been especially extensively studied in the context of $3d$ ionic crystals and polar semiconductors.^{2,3,4} The polaronic effect also grows with the confinement: the polaron binding energy E_b^{pol} in $2d$ is larger than in $3d$ and would diverge in pure $1d$.^{5,6} Various aspects of the excitonic and polaronic effects have been explored for many specific low-dimensional systems.

Of particular interest to us is a relationship between E_b^{exc} and E_b^{pol} , each of the binding energies understood as measured from the band edges in the absence of the polaronic effect. The ratio $E_b^{\text{pol}}/E_b^{\text{exc}}$ of the binding energies has a clear significance for the relative energetics of closely-bound and well-separated electron-hole pairs that is expected to affect practically important processes of charge separation and recombination. The bare value E_b^{exc} signifies the ionization energy, whether thermal or photo, required for “unbinding” of the exciton into well-separated band-edge electron and hole. In the presence of the polaronic effect, however, the thermal ionization

(dissociation) would occur into distant electron-polaron and hole-polaron so that the exciton thermal ionization energy is reduced from E_b^{exc} to $E_b^{\text{exc}} - 2E_b^{\text{pol}}$. We are interested in how much of this relative reduction might be possible to achieve due to the formation of *strong-coupling* (adiabatic) polarons. Our discussion here is restricted to systems with equal electron and hole effective masses so that the electron-polaron and hole-polaron have the same binding energies while the neutral exciton does not experience the adiabatic polaronic energy correction.^{7,8}

It is instructive to look at the ratio $E_b^{\text{pol}}/E_b^{\text{exc}}$ based on the results known for isotropic systems of “well-defined” dimensionality, that is, for purely $3d$, $2d$ and $1d$ systems. One would then find that, while each of the binding energies increases with more confinement, their growth occurs nearly “in proportion” so that the ratio does not change significantly. Indeed, classic Pekar’s result⁹ for $3d$ adiabatic polarons would translate into the maximum ratio of about 0.22. The exciton binding in $2d$ increases by a factor of 4 from its $3d$ value¹ but almost so does the polaron binding energy in $2d$ ⁵ resulting in the ratio $\simeq 0.20$. Moreover, if the divergent purely $1d$ binding energies are taken (parametrically) for their ratio, then the result of Ref. 6 would translate into maximum $E_b^{\text{pol}}/E_b^{\text{exc}}$ of approximately 0.17.

From the standpoint of this data, the results of our recent quasi- $1d$ calculations¹⁰ for polarons and excitons on nanotubes immersed in a $3d$ polar medium yielding $E_b^{\text{pol}}/E_b^{\text{exc}}$ in excess of 0.3 appear quite surprising. In the particular case of the tubular geometry, charge carriers are confined to the motion on a cylindrical surface. Our study¹⁰ was restricted to relatively small cylinder radii R . In this paper we will use a direct variational approach to calculate adiabatic polarons for arbitrary R thereby enabling an assessment of the evolution of the ratio $E_b^{\text{pol}}/E_b^{\text{exc}}$ between the purely $2d$ ($R \rightarrow \infty$) and quasi- $1d$ regimes. The corresponding calculations for excitons on a cylindrical surface have been performed

recently,^{11,12} which are very much in line with our excitation data. We will explicitly demonstrate (see Fig. 2(b)) that the ratio of the polaron and exciton binding energies exhibits a non-monotonic behavior as a function of the cylinder radius and can achieve as large values as about 0.35 at intermediate R where the cylinder circumference is roughly comparable to an appropriate Bohr radius. We believe that our demonstration of $E_b^{\text{pol}}/E_b^{\text{exc}}$ ratios above the values in purely $3d$ and $2d$ systems can be rationalized by invoking simple physical arguments. These arguments also suggest that the found *relative* increase of the polaronic effect may be reflective of a general behavior that might be characterized as a crossover effect.

Consider a gradual increase of the confinement, e. g., by starting to decrease the radius of a very large cylinder in going from the purely $2d$ system towards quasi- $1d$ or by starting to decrease the thickness of a very thick quantum well in going from the purely $3d$ system towards $2d$. Simplistically stated, the spatial size (extent) of a yet unconfined polaron wave function is larger than that of an unconfined exciton. As the confinement increases, therefore, the polaron can start experiencing a substantial growth of its binding energy due to the confinement before a “proportionally” substantial growth of the exciton binding energy sets in. With still further increase of the confinement, both polaron and exciton binding energies will be reflecting fuller confinement effects resulting in the corresponding trend of the decreasing ratio $E_b^{\text{pol}}/E_b^{\text{exc}}$. Of course, quantitative aspects of the evolution can vary for different systems and need to be evaluated accordingly. We also note that the above consideration tacitly assumed the existence of a uniform $3d$ polarizable medium with the confinement affecting only the motion of charge carriers. Strong violations of this assumption can significantly affect the outcome for the ratio of binding energies.

While serving as a suggestive illustration of a possibly general behavior, it is polarons and the relationship of polarons and excitons on a cylindrical surface that are the subjects of our direct interest in this paper. Organic and inorganic tubular (nano)structures attract a great deal of attention and are considered candidate systems for important applications like (photo)electrochemical energy conversion and (photo)catalytic production and storage of hydrogen as well as in optoelectronics. On one hand, their extended size along the tube axis can facilitate very good electron transport in that direction. On the other hand, tubes can expose large areas of both exterior and interior surfaces to facilitate surface-dependent reactions. Many of these applications involve contact with polar liquid environments such as common aqueous and non-aqueous solvents and electrolytic solutions which can provide conditions appropriate for the strong polaronic effect¹⁰ thereby changing the nature of charge carriers. A widely known example of the tubular geometry is single-walled carbon nanotubes (SWNTs) and, in fact, “chiral selective reactivity and redox chemistry of carbon nanotubes are two emerging fields of nanoscience”.¹³ We

note that the importance of the excitonic effects in the optics of semiconducting SWNTs is well established now with the radius R -dependent binding energies E_b^{exc} experimentally measured in some SWNTs to be in the range of 0.4 – 0.6 eV.^{14,15,16} There is also a growing evidence of the environmental effects on the electronic properties of SWNTs.^{17,18,19} The assumption of equal electron and hole effective masses is a good approximation for SWNTs.

It can be anticipated that the polaronic effect would have an influence both on charge-transfer reactions and charge carrier dynamics on the tubes. In the context of our discussion of the relative energetics, a substantial reduction of the activation energy due to the polaronic effect should be expected for electric-field-assisted exciton dissociation and charge separation on semiconducting nanotubes.

II. EXCITON AND POLARON ENERGY FUNCTIONALS

Following Refs. 11 and 12, the basic model we consider in this paper assumes that electron and hole are particles of the same effective mass $m_e = m_h = m$ whose motion is restricted to the surface of the cylinder of radius R . The cylindrical surface itself is immersed in the uniform $3d$ dielectric continuum characterized, as is common in studies of the polaron^{2,3,4} and solvation²⁰ effects, by two magnitudes of the dielectric permittivity: the high-frequency (optical) value of ϵ_∞ and the low-frequency (static) value of ϵ_s . In the case of liquid polar media, the slow component of the polarization is ordinarily associated with the orientational polarization of the solvent dipoles and it is typical^{10,20} that $\epsilon_s \gg \epsilon_\infty$. The fast component of the polarization follows charge carriers instantaneously. The slow component of the polarization, on the other hand, is considered static in the adiabatic picture to determine the electronic states; the slow component then responds to the averaged electronic charge distribution.

With $m_e = m_h$, there is no net charge density associated with the ground state of the neutral exciton that would cause a static polarization of the slow component (“non-polarizing exciton”). The Coulomb interaction between the electron and the hole in the exciton is screened only by the high-frequency dielectric response ϵ_∞ .^{7,8,21} The total energy of the exciton as a functional of the normalized wave function $\psi(\mathbf{r})$ of the electron-hole relative motion (reduced mass $m/2$) is then

$$\begin{aligned} \mathcal{E}^{\text{exc}}\{\psi\} &= K^{\text{exc}} - U^{\text{exc}} \\ &= \frac{\hbar^2}{m} \int d\mathbf{r} |\nabla\psi(\mathbf{r})|^2 - \frac{e^2}{\epsilon_\infty} \int d\mathbf{r} \frac{|\psi(\mathbf{r})|^2}{D(\mathbf{r})}, \quad (1) \end{aligned}$$

whose global minimum determines the exciton ground state wave function and its binding energy. For our geometry, position vector $\mathbf{r} = (x, y)$ is confined to the cylindrical surface, where we choose x to be along the cylinder axis and $-\pi R < y < \pi R$ along the circumferential

direction; $|\nabla\psi(\mathbf{r})|^2 = (\partial\psi/\partial x)^2 + (\partial\psi/\partial y)^2$. Coulomb interaction is determined by the physical distance in the $3d$ space; in the flat geometry it would be $D(\mathbf{r}) = |\mathbf{r}|$, for the points on the cylindrical surface

$$D(\mathbf{r}) = \left(x^2 + 4R^2 \sin^2 \frac{y}{2R}\right)^{1/2}. \quad (2)$$

Optimization of the functional (1) for the ground state of the exciton on a cylinder has been performed in Refs. 11 and 12 with the results in a very good agreement with our data to be used in the comparison with the polaron.

Polarons we discuss here are of the large-radius Fröhlich-Pekar type where the Coulomb field of an individual charge carrier supports a self-consistent dielectric polarization pattern surrounding the carrier. The formation of large-radius polarons (self-localization, self-trapping) occurs due to the interaction of charge carriers with the “slow” component of polarization. As the fast component of polarization does not contribute to the polaronic effect, it is the effective dielectric constant ϵ^* :

$$1/\epsilon^* = 1/\epsilon_\infty - 1/\epsilon_s, \quad (3)$$

that affects the coupling strength.^{2,3,4} In the adiabatic approximation, the normalized wave functions $\psi(\mathbf{r})$ of a self-localized charge carrier correspond to the minima of the following polaron energy functional:

$$\begin{aligned} \mathcal{E}^{\text{pol}}\{\psi\} &= K^{\text{pol}} - U^{\text{pol}} \\ &= \frac{\hbar^2}{2m} \int d\mathbf{r} |\nabla\psi(\mathbf{r})|^2 \\ &\quad - \frac{e^2}{2\epsilon^*} \int d\mathbf{r}_1 d\mathbf{r}_2 \frac{|\psi(\mathbf{r}_1)|^2 |\psi(\mathbf{r}_2)|^2}{D(\mathbf{r}_1 - \mathbf{r}_2)}, \end{aligned} \quad (4)$$

whose global minimum we will be seeking for the ground state of the polaron. The functional (4) is a result of the optimization of the total adiabatic energy functional with respect to the polarization of the medium thereby exhibiting an effective self-interaction of the electron.^{4,8,10} Correspondingly, the U^{pol} term in Eq. (4) is known to be “made of” two parts: $-U^{\text{pol}} = -U_{el}^{\text{pol}} + U_d^{\text{pol}}$, where U_{el}^{pol} represents the magnitude of the potential energy of the electron in the polarization field and U_d^{pol} the energy required to create this polarization (“deformation energy”); with the optimal polarization, $U_d^{\text{pol}} = U_{el}^{\text{pol}}/2$.

Both energy functionals (1) and (4) assume that the electron and hole energies are measured from the band edges.

It is convenient to factor out dependences on physically relevant combinations of parameters by introducing appropriate units of energy and length. We will choose such units based on combinations for the exciton Bohr radius and binding energy (effective Rydberg) in $3d$:

$$a_0 = 2e\hbar^2/me^2, \quad \text{Ry} = e^2/2\epsilon a_0. \quad (5)$$

For the exciton problem, Eq. (1), one uses $\epsilon = \epsilon_\infty$ in Eq. (5) and for the polaron problem, Eq. (4), it is $\epsilon = \epsilon^*$.

We use superscript indices “exc” and “pol” to distinguish between the corresponding units (5). With all the coordinates (x, y for the cylinder) measured in appropriate a_0 , one arrives at dimensionless energy functionals: $\mathcal{E}_0^{\text{exc}} = \mathcal{E}^{\text{exc}}/\text{Ry}^{\text{exc}}$ and $\mathcal{E}_0^{\text{pol}} = \mathcal{E}^{\text{pol}}/\text{Ry}^{\text{pol}}$, where

$$\mathcal{E}_0^{\text{exc}}\{\psi\} = \int d\mathbf{r} |\nabla\psi(\mathbf{r})|^2 - 2 \int d\mathbf{r} \frac{|\psi(\mathbf{r})|^2}{D_0(\mathbf{r})} \quad (6)$$

and

$$\mathcal{E}_0^{\text{pol}}\{\psi\} = \frac{1}{2} \int d\mathbf{r} |\nabla\psi(\mathbf{r})|^2 - \int d\mathbf{r}_1 d\mathbf{r}_2 \frac{|\psi(\mathbf{r}_1)|^2 |\psi(\mathbf{r}_2)|^2}{D_0(\mathbf{r}_1 - \mathbf{r}_2)}. \quad (7)$$

The dimensionless $D_0(\mathbf{r})$ in Eqs. (6) and (7) features the same behavior as Eq. (2) but with R replaced by the corresponding $R_0 = R/a_0$.

The global minima of Eqs. (6) and (7): $-E_0^{\text{exc}}$ and $-E_0^{\text{pol}}$, respectively, would determine the dimensionless binding energies. As units (5) already establish the scaling rules, in what follows we will be comparing E_0^{exc} and E_0^{pol} at the same values of R_0 . The ratio $E_0^{\text{pol}}/E_0^{\text{exc}}$ would have a direct physical meaning of maximum achievable when $\epsilon_s \gg \epsilon_\infty$ and $\epsilon^* \simeq \epsilon_\infty$ in Eq. (3). As we mentioned earlier, this can be a typical situation for many polar solvents.

Before proceeding with the analysis for a cylindrical surface, we recall in more detail benchmarks known for isotropic d -dimensional systems ($D_0(\mathbf{r}) = |\mathbf{r}| = r$) briefly described in the Introduction. The exact isotropic excitonic ground state $\psi(r)$ corresponding to Eq. (6) is given by the solution of the Schrödinger equation

$$-E_0^{\text{exc}}\psi = -\frac{\partial^2\psi}{\partial r^2} - \frac{(d-1)}{r} \frac{\partial\psi}{\partial r} - \frac{2}{r} \psi,$$

yielding well-known

$$\psi(r) \propto \exp\left(-\frac{2r}{d-1}\right), \quad E_0^{\text{exc}} = \frac{4}{(d-1)^2}. \quad (8)$$

With our choice of units, $E_0^{\text{exc}} = 1$ in $3d$.

The polaronic ground-state wave functions and energies corresponding to Eq. (7) are known from variational calculations for d -dimensional systems. It is customary in the polaronic literature to express energies in terms of the coupling constant $\alpha_c = (me^4/2\epsilon^*2\hbar^3\omega)^{1/2}$ and phonon frequency ω . Note that the combination $\alpha_c^2 \hbar\omega$ appearing in results for strong-coupling (adiabatic) polarons corresponds to 2Ry^{pol} as defined in Eq. (5). Thus well-known Pekar’s result⁹ for the $3d$ polaron translates into $E_0^{\text{pol}} \simeq 0.218$ and into the same magnitude of the ratio $E_0^{\text{pol}}/E_0^{\text{exc}}$ in $3d$.

The $2d$ polaron has been studied in great detail in Ref. 5 with the best result of $E_0^{\text{pol}} \simeq 0.809$ for the adiabatic case achieved with Pekar-type trial wave functions. Since $E_0^{\text{exc}} = 4$ in $2d$, the ratio $E_0^{\text{pol}}/E_0^{\text{exc}} \simeq 0.202$, only slightly smaller than in $3d$. The $2d$ case represents the

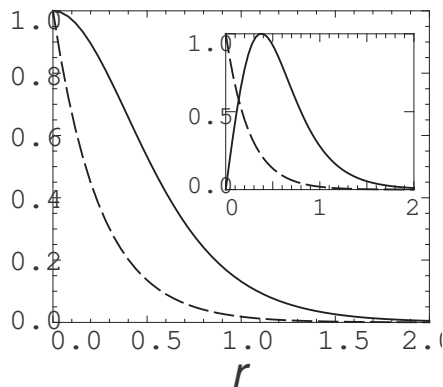


FIG. 1: The spatial distribution of unnormalized density $|\psi(r)|^2$ for the exciton (dashed line) and the polaron (solid line) in $2d$. The polaron wave function is as per Eq. (9). The inset shows the corresponding spatial distribution $U(r)$ of the potential energy in $U = \int U(r)dr$.

limit $R \rightarrow \infty$ for a cylindrical surface and is particularly important for our analysis. We have looked at simpler one-parametric trial wave functions that would make a good representation of the $2d$ adiabatic polaron and found that the wave function

$$\psi(r) \propto \frac{1}{\cosh(\alpha r)} \quad (9)$$

with $\alpha \simeq 1.674$ yields a very good optimization for the energy: $E_0^{\text{pol}} \simeq 0.804$, quite accurate for our purposes. Figure 1 compares the spatial structure of the $2d$ exciton and polaron.

As both exciton and polaron binding energies diverge in pure $1d$, the following comparison might be of a dubious nature but is still interesting. Specifically, Ref. 6 discussed the calculation of the $1d$ polaron in terms of the renormalized coupling constant $\alpha'_c = \alpha_c/(d-1)$, where $d \rightarrow 1$. The best variational result achieved for the adiabatic polaron was $E_b^{\text{pol}} \simeq 0.333 (\alpha'_c)^2 \hbar\omega$. As the diverging d -dependence in this expression is the same $(d-1)^{-2}$ as in the exciton case (8), the ratio of the binding energies in $1d$ could then be interpreted as $E_0^{\text{pol}}/E_0^{\text{exc}} \simeq 0.167$.

III. VARIATIONAL ANALYSIS FOR A CYLINDER

When on a cylindrical surface, both exciton and polaron ground states need to be determined numerically. Our variational analysis of the energy functionals (6) and (7) has been performed on the following classes of the trial wave functions.²⁸ For the exciton problem we have used three-parametric (α , β and γ) wave functions

$$\psi(x, y) \propto \exp \left[-(\alpha^2 x^2 + \beta^2 y_1^2 + \gamma^2)^{1/2} \right]. \quad (10)$$

The polaron problem is much more computation time demanding and we chose two-parametric (α and β) wave

functions

$$\psi(x, y) \propto \frac{1}{\cosh(\alpha^2 x^2 + \beta^2 y_1^2)^{1/2}}. \quad (11)$$

The functional dependences in Eqs. (10) and (11) are such that they can recover, in the limit of $R_0 \rightarrow \infty$, wave functions (8) and (9) found for the $2d$ systems – similarly to the earlier exciton calculations.^{11,12}

We explored two choices for the effective coordinate y_1 in Eqs. (10) and (11): “arc-based” (as in Ref. 12)

$$y_1 = y, \quad (12)$$

– $\pi R_0 < y < \pi R_0$, and “chord-based” (as in Ref. 11)

$$y_1 = 2R_0 \sin(y/2R_0). \quad (13)$$

Both choices can be thought of as respectively $n \gg 1$ and $n = 1$ limits of more general

$$y_1 = \pi R_0 \left\{ \frac{2}{\pi} \sin \left[\frac{\pi}{2} \left(\frac{y}{\pi R_0} \right)^n \right] \right\}^{1/n}$$

that could be used in future refinements as being more flexible in terms of the shape of the wave function periodic in the circumferential direction. In this paper we resorted to just choosing the best results among obtained with Eqs. (12) and (13).

Wave functions (10) and (11) feature two parameters α and β having the meaning of inverse lengths thereby explicitly allowing for anisotropy of the wave function extent in the axial and circumferential directions.¹² What we will later be referring to as quasi- $1d$ results corresponds to $\beta = 0$ when the wave functions are uniform around the cylinder circumference.

Main quantitative results of this paper are displayed in Figure 2 showing the optimized variational outputs for the exciton and polaron binding energies as well as their ratio $E_0^{\text{pol}}/E_0^{\text{exc}}$. Our exciton data is very close to results of Refs. 11 and 12 where the reader can find extensive discussions.

Just as in the exciton case, the polaron binding energy exhibits very little change from its $2d$ value ($\simeq 0.8$) due to the curvature up to $R_0 \sim 1$ (see the inset in Fig. 2(a)) where it starts rising, relatively earlier and more rapidly than the exciton dependence. This immediately translates into a substantial increase of the ratio $E_0^{\text{pol}}/E_0^{\text{exc}}$ with decreasing R_0 as shown in Fig. 2(b). The maximum of the ratio $\simeq 0.35$ is achieved in the region of $1/R_0 \sim 10$, after which the ratio starts slowly decreasing with $1/R_0$. While, of course, larger ratios $E_0^{\text{pol}}/E_0^{\text{exc}}$ lead to larger relative reductions of the effective activation energy $E_0^{\text{exc}} - 2E_0^{\text{pol}}$, it is quite interesting that the *absolute* value of this activation energy, also shown in Fig. 2(b), exhibits a non-monotonic dependence on $1/R_0$. A region around the minimum of this curve indicates specific tube sizes where the activation energy would be at its lowest.

Our variational results have shown that the dependence of E_0^{pol} on $1/R_0$ collapses onto the corresponding

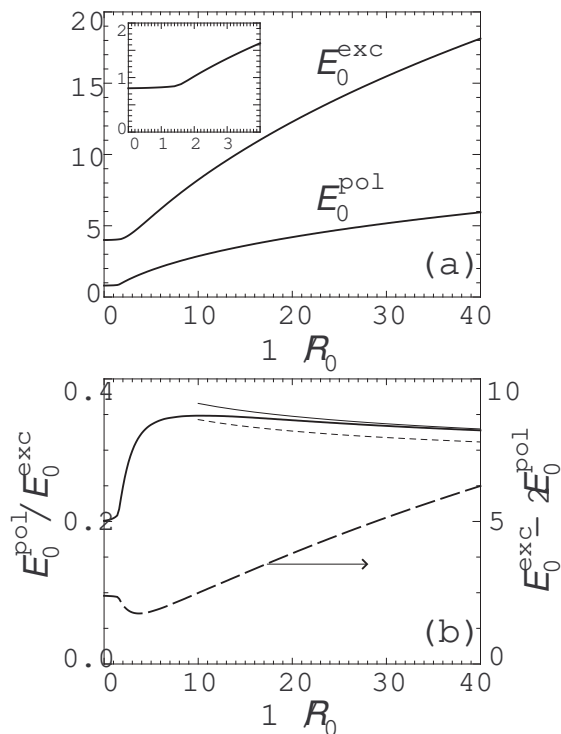


FIG. 2: (a) The dimensionless exciton and polaron binding energies as functions of the dimensionless inverse cylinder radius $1/R_0$. The inset shows the behavior of the polaron binding energy in more detail at small $1/R_0$. (b) The ratio of the binding energies $E_0^{\text{pol}}/E_0^{\text{exc}}$ of the excitations on a cylinder is shown as a thick solid line. A thin solid line displays this ratio as it is obtained in the quasi-1d calculation with the effective tube potential (15). A thin short-dash line shows the quasi-1d result for this ratio if the effective interaction, instead, was that of a quantum wire, Eq. (16). A thick long-dash line displays the dimensionless activation energy $E_0^{\text{exc}} - 2E_0^{\text{pol}}$.

quasi-1d curve practically right away after the onset of a substantial rise in the binding. This is different from the exciton case where deviations from the quasi-1d behavior persist all the way into the region of $1/R_0 > 20$. In other words, the polaron spreads uniformly around the cylinder at much smaller curvatures than the exciton does. We note that the quasi-1d variational results for the polaron binding using trial wave functions (11) and (10) differ very little and are in good agreement with our analysis in Ref. 10 where no assumptions have been made about the wave function shape and the nonlinear optimizing equation has been solved numerically. The thin solid line in Fig. 2(b) shows the ratio $E_0^{\text{pol}}/E_0^{\text{exc}}$ using quasi-1d results for the binding energies and its deviation from the variational result for a cylinder is entirely due to underestimation of the exciton binding.

As with all variational calculations, we, of course, cannot exclude that some details in the results shown in Fig. 2 may undergo slight modifications upon further improvements of variational wave functions. Importantly,

possible improvements would be inconsequential for our main observations of a non-monotonic dependence of the ratio $E_0^{\text{pol}}/E_0^{\text{exc}}$ on $1/R_0$ and of the magnitude of the ratio reaching values well above the 2d value of $\simeq 0.2$. We found that a rise of the ratio above 0.3 is obtainable even if the polaron wave functions are not specifically optimized for a range of given R_0 but the 2d optimal values of $\alpha = \beta \simeq 1.67$ are used. For very small tubes with $1/R_0 \gtrsim 20$, results of exact numerical calculations in Ref. 10 complement the picture.

The transitional region of $R_0 \sim 1$ is likely to be especially sensitive to the choice of trial wave functions. So Ref. 11 reported a few-percent improvement for the exciton binding energy in the region of $1 \lesssim 1/R_0 \lesssim 2.5$ with certain trial functions. Similar improvements could perhaps be found for the polaron binding energies. Figure 3 illustrates the behavior of the polaron functional (7) in the transitional region, at $R_0 = 0.65$, as a function of the variational parameters α and β . A curious feature of the “landscape” in Fig. 3(a) is a clear coexistence of two minima, one corresponding to a polaronic state that is uniformly distributed (delocalized) around the cylinder circumference, and the other where the circumferential distribution is non-uniform. While this appears as an interesting possibility, it could as well be an artefact of a restricted nature of a specific class of the trial wave functions, compare, e.g., visually to the landscape of Fig. 3(b). A much more careful study would be needed to explore the possibility of coexisting polaronic states requiring an analysis of actual adiabatic potential surfaces. An example of an analogous analysis can be found in Ref. 22, where we proved a coexistence of different polarons in certain quasi-1d systems.

IV. DISCUSSION

Both in this paper and in Ref. 10 we have shown that the strong polaronic effect occurring in sluggish polar environments substantially affects the relative energetics of closely-bound and well-separated electron-hole pairs on a cylindrical surface of nanotubes. The binding energy E_b^{pol} of an individual polaron can, in principle, reach as much as about 0.35 of the binding energy E_b^{exc} of the exciton. This would translate into a reduction of the activation energy $E_b^{\text{exc}} - 2E_b^{\text{pol}}$ for exciton dissociation by a factor of about 3 from the value E_b^{exc} it would have in a non-polar environment with the same value of the high-frequency dielectric constant ϵ_∞ . Note that we have not found any additional energy barriers between the exciton and distant polaron-pair states.¹⁰ One should expect that enhanced separation of charges and a corresponding luminescence quenching would then result, e.g., in experiments probing electric field effects on the luminescence. Needless to say that additional factors can make the reduction magnitude we discussed smaller, see, e.g., a comparison in Ref. 10 of cases with different “electrostatic conditions”.

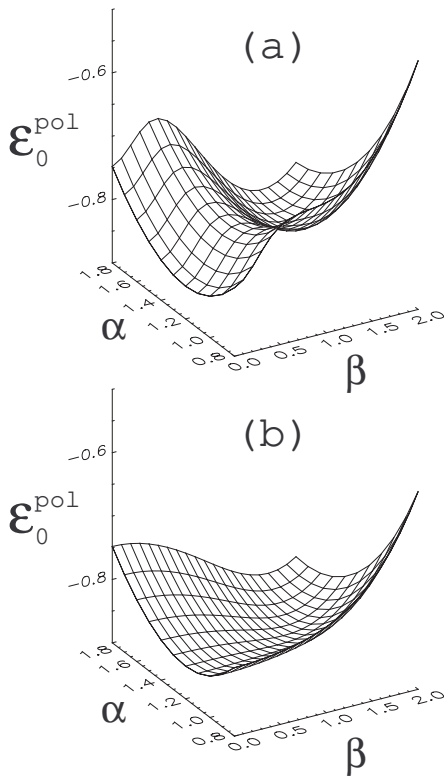


FIG. 3: The behavior of the functional (7) at $R_0 = 0.65$ with the trial wave functions (11) as a function of the variational parameters α and β for two choices of the effective coordinate y_1 : (a) as in Eq. (12) and (b) as in Eq. (13).

Polar liquid environments such as many common solvents may be good candidates to provide conditions necessary for the strong polaronic effect as they can exhibit both high values of the static dielectric constant ϵ_s and a relatively slow response of the orientational polarization (longitudinal relaxation times can be on the order of 1 ps and longer)^{10,20}. Quite befittingly, there is an intense ongoing research effort on various applications of nanotubes in contact with such environments and we hope that direct experimental verifications of our conclusions would be possible. We note that a comprehensive mapping of luminescence versus absorption spectra of individual SWNTs was in fact achieved in aqueous suspensions.^{23,24} Interestingly, numerical estimates in Ref. 12 indicate that the dimensionless radius R_0 for a range of SWNTs may be close to 0.1, which corresponds to the region of maximum $E_0^{\text{pol}}/E_0^{\text{exc}}$ ratios in Fig. 2(b).

We have demonstrated that the ratio of the binding energies $E_b^{\text{pol}}/E_b^{\text{exc}}$ has a non-monotonic dependence on the cylinder curvature $1/R$. As argued in the Introduction, our particular observation for the cylindrical geometry can be a manifestation of a more general crossover effect that would be common for other structures in $3d$ polar media when the increasing confinement of the electron motion causes a “transition” between d -dimensional systems, such as between $3d$ and $2d$ (quantum wells) or

between $3d$ and $1d$ (quantum wires). Basically, the origin of this effect can be related to the fact that the spatial extent of an unconfined polaron is larger than the size of an unconfined exciton (see Fig. 1 for the $2d$ case) thereby making the polaron “respond” to the initially increasing confinement in a more pronounced way than the exciton. Only after the exciton experiences a fuller effect of the confinement, the ratio of the binding energies starts decreasing. Elaborating more on this idea, the inset in Fig. 1 shows the spatial distribution of the potential energy terms U : $\mathcal{E} = K - U$, for unconfined excitations. It is evident that the “longer-range” contributions to the polaron potential energy are relatively more important than for the exciton. That is why the effect of the increasing confinement on the polaron is initially relatively stronger. In the particular case of the cylindrical geometry, the curvature changes remote physical distances (chords instead of arcs, Eq. (2)) more than it does close distances.

A meaningful parallel can be drawn with the behavior of the ratio U/K of the potential and kinetic energy terms in confined systems. Virial theorem for the Coulombically bound states in unconfined d -dimensional systems states that $U/K = 2$ independently of d , which, of course, also follows directly from scaling of both functionals (1) and (4) provided that $D(\mathbf{r}) = |\mathbf{r}| = r$. Particularly, polarons in such systems are known^{4,8,25} to satisfy the following ratios for various energy terms: $E_b^{\text{pol}} : K^{\text{pol}} : U^{\text{pol}} : U_{el}^{\text{pol}} : U_d^{\text{pol}} = 1 : 1 : 2 : 4 : 2$. Some of these relationships are violated in confined systems. As studied in Ref. 26, the virial theorem ratio $U^{\text{exc}}/K^{\text{exc}}$ for excitons in quantum wells and quantum wires is larger than 2 and, in fact, a non-monotonic dependence of $U^{\text{exc}}/K^{\text{exc}}$ has been demonstrated for quantum wells transitioning between $3d$ and $2d$ limits. We have found a non-monotonic behavior of the ratio U/K for both polarons and excitons on a cylinder as a function of the curvature $1/R$. In agreement with our qualitative arguments, at smaller $1/R$, this ratio grows much faster for the polaron than for the exciton. At large curvatures, however, the trend is reversed and the exciton has larger ratios U/K than the polaron.

It is useful to continue a qualitative reasoning by discussing the quasi- $1d$ limit of our results, that is, the case of stronger but still finite degrees of confinement. One can then use the notion of the effective Coulomb potentials,^{1,26} here as a function of the $1d$ (axial) distance x . (The effective Coulomb potentials for $2d$ can be similarly introduced.²⁶) Figure 4 compares three potentials in units such that at very large distances the potentials behave as

$$V_{\text{eff}}(x) = R_0/x. \quad (14)$$

In this limit the electron wave function is delocalized around the tube circumference and the effective inter-

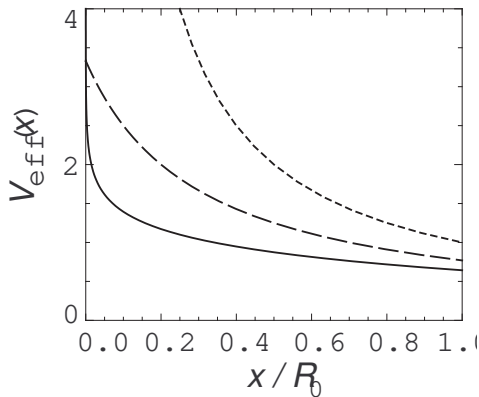


FIG. 4: Distance dependence of the effective 1d Coulomb potentials for charges on a cylinder, Eq. (15), solid line, and in a quantum wire, Eq. (16), long-dash line, in comparison with the original Coulomb interaction (14), short-dash line.

action becomes that of rings of charge given by

$$V_{\text{eff}}(x) = \frac{2}{\pi [(x/R_0)^2 + 4]^{1/2}} K \left[\frac{4}{(x/R_0)^2 + 4} \right], \quad (15)$$

where $K(m) = \int_0^{\pi/2} (1 - m \sin^2 \theta)^{-1/2} d\theta$ is a complete elliptic integral of the first kind. If, instead of a tube, we dealt with a quantum wire, the electron wave function would be delocalized throughout the cross-section of the wire with the effective interaction approximated as¹

$$V_{\text{eff}}(x) = \frac{1}{(x/R_0) + 0.3}. \quad (16)$$

Both effective tube (15) and wire (16) 1d potentials feature modifications of the shorter-range interaction from the original Coulomb (14) due to the transverse spread of wave functions thereby eliminating a pure 1d divergence of the ground states for excitons and polarons. As we discussed above, the role of the longer-distance interactions is more important for the polaron than for the exciton. Since the relative modification of the original Coulomb to the effective potentials is increasing towards shorter distances, it is then clear that the ratio $E_b^{\text{pol}}/E_b^{\text{exc}}$ in systems with modified interactions should be larger than values around 0.2 in systems with the pure Coulomb interaction. Moreover, following the same logic, one should expect that the larger modification is from the original Coulomb to the effective potentials the larger would be $E_b^{\text{pol}}/E_b^{\text{exc}}$ ratios. Figure 4 shows that deviations from the Coulomb dependence for the effective wire potential are smaller than for the tube potential (over a relevant spatial range). We have performed a quasi-1d variational optimization of the polaron and exciton binding energies with the tube potential (15). The resulting ratios $E_0^{\text{pol}}/E_0^{\text{exc}}$ are shown in Fig. 2(b) with a short-dash thin line and indeed smaller than the ratios calculated with the tube potential (15), solid thin line in that figure.

Our qualitative arguments, while confirmed by specific calculations, do not appear to be restricted to this specific situation. We therefore believe that findings of larger magnitudes of the ratio $E_b^{\text{pol}}/E_b^{\text{exc}}$ and of a non-monotonic dependence of this ratio on the degree of confinement represent a crossover effect that can be common to semiconductor nanostructures in 3d polar environments. Further calculations with different structures are needed to validate this conjecture and evaluate its quantitative aspects, including in non-uniform polar environments.

Another important venue for future research is an assessment of the activation energy for exciton dissociation in confined semiconductors with unequal electron and hole masses, $m_e \neq m_h$. In this case electron- and hole-polarons have different binding energies and, in addition, the exciton itself can cause an adiabatic polarization of the environment.^{7,21} The corresponding “polaronic” corrections to the exciton binding in quantum-well wires have, e.g., been studied in Ref. 27. From a general standpoint, one would also like to extend the analysis of the effects of polar media on the dissociation of confined excitons to the intermediate-coupling^{2,3,4} case.

Acknowledgments

We are deeply grateful to V. M. Agranovich for many useful discussions. This study contributes to a project supported by the Collaborative U. T. Dallas – SPRING Research and Nanotechnology Transfer Program. The work of SOC was supported by the University of Texas at Dallas Summer Research Program.

-
- ¹ H. Haug and S. W. Koch, *Quantum theory of the optical and electronic properties of semiconductors* (World Scientific, New Jersey, 2004).
 - ² H. Fröhlich, *Adv. Phys.* **3**, 325 (1954).
 - ³ C. G. Kuper and G. D. Whitfield, eds., *Polarons and excitons* (Plenum, New York, 1963).
 - ⁴ J. Appel, in *Solid State Physics*, edited by F. Seitz, D. Turnbull, and H. Ehrenreich (Academic, New York, 1968), vol. 21, p. 193.
 - ⁵ X. Wu, F. M. Peeters, and J. T. Devreese, *Phys. Rev. B* **31**, 3420 (1985).
 - ⁶ F. M. Peeters and M. A. Smondyrev, *Phys. Rev. B* **43**, 4920 (1991).
 - ⁷ I. M. Dykman and S. I. Pekar, *Dokl. Akad. Nauk SSSR* **83**, 825 (1952).
 - ⁸ E. I. Rashba, in *Excitons. Selected chapters*, edited by E. I. Rashba and M. D. Sturge (North Holland, Amsterdam, 1987), p. 273.
 - ⁹ S. I. Pekar, *Zh. Eksp. Teor. Fiz.* **16**, 335, 341 (1946).
 - ¹⁰ Y. N. Gartstein, *Phys. Lett. A* **349**, 377 (2006).
 - ¹¹ M. K. Kostov, M. W. Cole, and G. D. Mahan, *Phys. Rev. B* **66**, 075407 (2002).
 - ¹² T. G. Pedersen, *Phys. Rev. B* **67**, 073401 (2003).
 - ¹³ M. J. O'Connell, E. E. Eibergen, and S. K. Doorn, *Nature Materials* **4**, 412 (2005).
 - ¹⁴ F. Wang, G. Dukovic, L. E. Brus, and T. F. Heinz, *Science* **308**, 838 (2005).
 - ¹⁵ Y.-Z. Ma, L. Valkunas, S. M. Bachilo, and G. R. Fleming, *J. Phys. Chem. B* **109**, 15671 (2005).
 - ¹⁶ Z. Wang, H. Pedrosa, T. Krauss, and L. Rothberg, *Phys. Rev. Lett.* **96**, 047403 (2006).
 - ¹⁷ C. Fantini, A. Jorio, M. Souza, M. S. Strano, M. S. Dresselhaus, and M. A. Pimenta, *Phys. Rev. Lett.* **93**, 147406 (2004).
 - ¹⁸ T. Hertel, A. Hagen, V. Talalaev, K. Arnold, F. Hennrich, M. Kappes, S. Rosenthal, J. McBride, H. Ulbricht, and E. Flahaut, *Nano Lett.* **5**, 511 (2005).
 - ¹⁹ M. P. Lu, C. Y. Hsiao, P. Y. Lo, J. H. Wei, Y. S. Yang, and M. J. Chen, *Appl. Phys. Lett.* **88**, 053114 (2006).
 - ²⁰ W. R. Fawcett, *Liquids, solutions and interfaces* (Oxford, Oxford, 2004).
 - ²¹ S. I. Pekar, E. I. Rashba, and V. I. Sheka, *Sov. Phys. JETP* **49**, 129 (1979).
 - ²² Y. N. Gartstein and A. A. Zakhidov, *Solid St. Commun.* **60**, 105 (1986).
 - ²³ M. J. O'Connell, S. M. Bachilo, C. B. Huffman, V. C. Moore, M. S. Strano, E. H. Haroz, K. L. Rialon, P. J. Boul, W. H. Noon, C. Kittrell, et al., *Science* **297**, 593 (2002).
 - ²⁴ R. B. Weisman, S. M. Bachilo, and D. Tsyboulski, *Appl. Phys. A* **78**, 1111 (2004).
 - ²⁵ S. I. Pekar, *Research in the electron theory of crystals* (Gostekhizdat, Moscow, 1951).
 - ²⁶ Y. Zhang and A. Mascarenhas, *Phys. Rev. B* **59**, 2040 (1999).
 - ²⁷ M. H. Degani and O. Hipólito, *Phys. Rev. B* **35**, 9345 (1987).
 - ²⁸ All numerical integrations and optimizations have been done by using IMSL numerical libraries as provided with the PV-WAVE Advantage package, <http://www.vni.com>.